

OC kappa increases in the levels of glucose, trehalose, TOR-P and transcripts encoding proteins involved in photosynthesis, and basal and secondary metabolisms in *Eucalyptus globulus*

Silvia Saucedo¹, Alberto González², Melissa Gómez², Rodrigo A Contreras², Daniel Laporte², Claudio A Sáez³, Gustavo Zúñiga², Alejandra Moenne^{Corresp. 2}

¹ Facultad de Ciencias Agrarias, Universidad Técnica Estatal de Quevedo, Quevedo, Ecuador

² Department of Biology, Faculty of Chemistry and Biology, Universidad de Santiago de Chile, Santiago, Chile

³ Center for Advanced Studies, Universidad de Playa Ancha, Viña del Mar, Chile

Corresponding Author: Alejandra Moenne
Email address: alejandra.moenne@usach.cl

Oligo-carrageenan (OC) kappa increases net photosynthesis, and basal and secondary metabolism enzyme activities in *Eucalyptus globulus* trees. Here, trees were sprayed on leaves with water (control) or with OC kappa 1 mg ml⁻¹, once a week, four times in total, and cultivated for 17 additional weeks (21 weeks in total). Height, level of glucose, trehalose, TOR phosphorylated in Ser2448 (TOR-P) and transcripts encoding TOR and S6 kinase (S6K) as well as the level of transcripts encoding proteins and enzymes involved in glucose accumulation, photosynthesis, C, N and S assimilation, and synthesis of phenylpropanoid compounds (PPCs) and terpenes were determined. Treated trees showed an increase in height of 105% compared to controls at week 21. Treated trees showed an increase in glucose and trehalose level having an oscillatory pattern with maximal levels for glucose at week 1, 9-11 and 17-19, and for trehalose at weeks 1-3, 5, 8-9, 12, 15-16 and 18-21. TOR-P showed increases from week 1 until the end of the experiment with peaks at weeks 2, 6, 12 and 16. The level of *tor* transcripts showed peaks at weeks 3, 6, 10-11 and 13 whereas the level of *s6k* transcripts remained unchanged. In addition, transcripts encoding proteins involved in photosynthesis, and enzymes involved in glucose accumulation, C, N and S assimilation, and synthesis of secondary metabolites showed an oscillatory pattern with increases mainly at weeks 3-4, 5-6, 10-11, and in some cases at weeks 13-14 and 16-18. Thus, the increases in trehalose levels better correlate with increases in TOR-P and transcript levels. Therefore, OC kappa induced an increase in the levels of glucose, trehalose, TOR-P and expression of genes involved in photosynthesis, and basal and secondary metabolism which may explain, at least in part, the increase in growth and defense responses in *E. globulus* trees.

1 **OC kappa increases in the levels of glucose, trehalose, TOR-P and transcripts**
2 **encoding proteins involved in photosynthesis, and basal and secondary**
3 **metabolisms in *Eucalyptus globulus***

4 **S. Saucedo^{1,2}, A. González¹, M. Gómez¹, R. A. Contreras¹, D. Laporte¹, C.A. Sáez³, G.**
5 **Zúñiga¹ and A. Moenne^{1,4}**

6 ¹Faculty of Chemistry and Biology, University of Santiago of Chile

7 ²Facultad de Ciencias Agrarias, Universidad Técnica Estatal de Quevedo, Quevedo, Ecuador

8 ³Laboratory of Coastal Environmental Research, Center of Advanced Studies, University of Playa
9 Ancha, Viña del Mar, Chile

10 ⁴ Corresponding author (alejandra.moenne@usach.cl)

11 **Keywords** basal metabolism, *Eucalyptus globulus*, glucose, growth, OC kappa, secondary
12 metabolism, TOR kinase, trehalose.

13 Abstract

14 Oligo-carrageenan (OC) kappa increases net photosynthesis, and basal and secondary metabolism
15 enzyme activities in *Eucalyptus globulus* trees. Here, trees were sprayed on leaves with water
16 (control) or with OC kappa 1 mg ml⁻¹, once a week, four times in total, and cultivated for 17
17 additional weeks (21 weeks in total). Height, level of glucose, trehalose, TOR phosphorylated in
18 Ser2448 (TOR-P) and transcripts encoding TOR and S6 kinase (S6K) as well as the level of
19 transcripts encoding proteins and enzymes involved in glucose accumulation, photosynthesis, C,
20 N and S assimilation, and synthesis of phenylpropanoid compounds (PPCs) and terpenes were
21 determined. Treated trees showed an increase in height of 105% compared to controls at week 21.
22 Treated trees showed an increase in glucose and trehalose level having an oscillatory pattern with
23 maximal levels for glucose at week 1, 9-11 and 17-19, and for trehalose at weeks 1-3, 5, 8-9, 12,
24 15-16 and 18-21. TOR-P showed increases from week 1 until the end of the experiment with
25 peaks at weeks 2, 6, 12 and 16. The level of *tor* transcripts showed peaks at weeks 3, 6, 10-11 and
26 13 whereas the level of *s6k* transcripts remained unchanged. In addition, transcripts encoding
27 proteins involved in photosynthesis, and enzymes involved in glucose accumulation, C, N and S
28 assimilation, and synthesis of secondary metabolites showed an oscillatory pattern with increases
29 mainly at weeks 3-4, 5-6, 10-11, and in some cases at weeks 13-14 and 16-18. Thus, the increases
30 in trehalose levels better correlate with increases in TOR-P and transcript levels. Therefore, OC
31 kappa induced an increase in the levels of glucose, trehalose, TOR-P and expression of genes
32 involved in photosynthesis, and basal and secondary metabolism which may explain, at least in
33 part, the increase in growth and defense responses in *E. globulus* trees.

34 Introduction

35 It is now well known that growth and development in mammals, nematodes yeast, plants and
36 algae is controlled by the kinase Target of Rapamycin (TOR) (Xiong and Sheen, 2015; Rexin et
37 al., 2015; Dobrenel et al., 2016). TOR is a phosphoinositol-related kinase (PIK) having
38 serine/threonine protein kinase activity and is a key regulatory kinase of the TOR pathway (Xiong
39 and Sheen, 2015; Rexin et al., 2015; Dobrenel et al., 2016). TOR kinase is large protein
40 constituted by several domains: a N-terminal Huntingtin, Elongation Factor 3, Regulatory
41 Subunit A of PPA2, TOR1 (HEAT) domain containing several HEAT repeats which are
42 constituted by 37-47 amino acids forming two α -helices and a solenoid structure that is
43 involved in protein-protein interactions and interaction with Regulatory-Associated Protein of
44 mTOR (RAPTOR) (Kim et al., 2002; Mahfouz et al., 2006). Contiguous to HEAT domain, is
45 FRAP, ATM; TTRAP (FAT) domain that is present in most PIK and is involved in protein-protein
46 interactions (Bosotti et al., 2000). Contiguous to FAT domain is FRB FKBP-Rapamycin-Binding
47 (FRB) domain that binds to FKBP12-rapamycin complex (Banaszynski et al., 2005; Rodriguez-
48 Camarzo et al., 2012). Contiguous to FRB domain is the catalytic domain (CD) that interacts with
49 Lethal with SEC13 protein 8 (LST8) regulatory protein (Schalm et al., 2003) and two TOR-LST8
50 complexes form a dimer mediated by TOR-TOR interactions (Baretic et al., 2016). Contiguous to
51 CD, is the C-terminal FAT domain (FATC) that is redox-sensitive and binds to membranes
52 (Takahashi et al., 2000; Dames, 2010). In mammals, TOR kinase is inhibited by nanomolar
53 concentrations of the macrolide rapamycin produced by the bacteria *Streptomyces hygroscopicus*
54 (Crespo et al., 2005). In contrast, plant TOR kinases are only moderately sensitive to rapamycin
55 (Ren et al., 2011; Ren et al., 2012). In this respect, it has been shown that when FKBP12, a prolyl
56 isomerase, is overexpressed or replaced by human or yeast FKBP12 in *Arabidopsis thaliana*,
57 TOR kinase becomes sensitive to rapamycin (Sormani et al., 2017; Xiong and Sheen, 2012).

58 In mammals, TOR is a large protein of around 280 kDa that is activated by phosphorylation
59 in Treo 2446, Ser 2448, Ser 2481 and Ser1261 (Chiang and Abraham, 2005; Acosta et al., 2009).
60 TOR pathway is activated by growth factors, pro-inflammatory cytokines, insulin, glucose, amino
61 acids as glutamine and leucine, and lipids; the latter leads to an increase in anabolic reactions,
62 cell division and growth (Jewell et al., 2015). In mammals, there is single gene encoding TOR,
63 although TOR kinase can interact with proteins RAPTOR, LST8 and FKBP12 to form complex
64 TORC1, which is sensitive to rapamycin, and it can also interact with RICTOR, LST8 and SIN1,
65 to form TORC2, which is insensitive to rapamycin (Sarbasov et al., 2004; Sarbasov et al., 2005;

Wullschelger and Loewith, 2006). TORC1 regulates the equilibrium among anabolism and catabolism, cell proliferation and temporal growth whereas TORC2 modulates cytoskeleton structure, spatial cell growth, cell polarity and apoptosis (Wullschelger and Loewith, 2006; Martin and Hall, 2005).

In plants, TOR is a protein of around 250 kDa, 39% identical in its amino acid sequence to human TOR (Dobrenel et al., 2016) and TOR is phosphorylated in Ser2448 since antibodies anti-human TOR-P Ser2448 recognize phosphorylated TOR (TOR-P) in cells of maize callus (Garrocho-Villegas et al., 2013). In addition, it has been shown that insulin-like growth factors (IGF) and bovine insulin promote growth in maize cells which correlates with the increase in the level of TOR-P. On the other hand, rapamycin inhibits IGF-induced growth stimulation as well as TOR phosphorylation in Ser 2448 (Garrocho-Villegas et al., 2013). In plants, TOR kinase interacts with RAPTOR, LST8 and rapamycin-FKBP12 (Dobrenel et al., 2016; Mahfouz et al., 2006; Garrocho-Villegas et al., 2013). TOR pathway in plants is activated by glucose, sucrose and amino acids, among others (Dobrenel et al., 2016; Ren et al., 2012). On the other hand, TOR is inhibited by the kinase SnRK1 that phosphorylates RAPTOR leading to inhibition of TOR kinase activity (Nukarinen et al., 2016). In turn, snRK1 is directly inhibited by glucose-6-P (G6P) and trehalose-6-P (T6P) (Toroser et al., 2000; Zhang et al., 2009). Thus, the increase in glucose and trehalose may lead to an increase in G6P and T6P and the inhibition of snRK1 resulting in the activation TOR kinase, and the stimulation of growth and development in plants.

It has been shown that activation of TOR pathway increases growth mainly by activating cell division through phosphorylation of E2Fa and E2Fb transcription factors (Xiong and Sheen, 2013), and by activating protein translation through phosphorylation of S6 kinase (S6K) that, in turn, phosphorylates the ribosomal small subunit 6 (Xiong and Sheen, 2013). More recently, it has been demonstrated that activation of TOR pathway in *A. thaliana* results in an increased expression of genes coding for enzymes involved in anabolic reactions, such as those related to the syntheses of proteins, amino acids, RNA, DNA and cell wall, as well as synthesis of enzymes involved in glycolysis, TCA cycle and proteins of mitochondrial electron transport chain (Ren et al., 2012; Xiong and Sheen, 2013; Caldana et al., 2013). Moreover, the inhibition of TOR pathway using the inhibitor of TOR kinase AZD8055 leads to a decrease in transcripts encoding proteins involved in photosynthesis, chlorophyll synthesis and C assimilation (Montane and Menand, 2013; Dong et al., 2015) indicating that the activation of TOR pathway leads to the increase photosynthesis and basal metabolism. Furthermore, the activation of TOR pathway down-regulates expression of genes coding for catabolic enzymes involved in protein, amino

acids, lipid syntheses, and related to starch degradation, autophagy and glyoxylate cycle (Xiong et al., 2013). In addition, activation of TOR pathway also increased the expression of genes coding for enzymes involved in secondary metabolism and defense responses, such as those that synthesize glucosinolates (Xiong et al., 2013). Similarly, TOR pathway mediates the increase in the level of phenylpropanoid compounds (PPCs) and glucosinolates in *A. thaliana* (Caldana et al., 2013). It has been recently shown that inhibition of TOR pathway with AZD8055 down-regulates the synthesis and signaling of phytohormones such as auxin, gibberelins, cytokinines and brassinosteroids (Dong et al., 2015; Deng et al., 2016), indicating that activation of TOR pathway also increase the synthesis of growth-promoting hormones.

On the other hand, marine algae oligo-carrageenans (OCs) enhance growth and defense responses in terrestrial plants (Moenne et al., 2016). OCs kappa, lambda and iota are obtained by acid hydrolysis of pure carrageenans kappa, lambda and iota, respectively, and displayed a DP=20-25 (Vera et al., 2011). It was initially determined that OCs kappa, lambda and iota applied on plant leaves at a concentration of 1 mg mL⁻¹, once a week, four times in total, mediated an increase in height and plant biomass in tobacco plants (var. Xhanti) cultivated in control conditions as well as tobacco plants (var. Burley) cultivated in the field for four months (Castro et al., 2012). In addition, OCs kappa, lambda and iota applied at a concentration of 1 mg mL⁻¹, once a week, four times in total, induced and increase in height, trunk diameter, net photosynthesis, and in the levels of PPCs and essential oils in *Eucalyptus globulus* cultivated in the field for three years (González et al., 2013b). On the other hand, it was shown that OC kappa mediated an increase in the synthesis of reducing compounds such as NADPH, ascorbate (ASC), and glutathione (GSH), as well as increased activities of thioredoxin reductase and thioredoxin in *E. globulus* trees cultivated for four months outdoors. In addition, OC kappa increases the activity of enzymes involved basal metabolism, C, N and S assimilation, purine and pyrimidine syntheses, and in the activities of Krebs cycle enzymes (González et al., 2014a). Furthermore, in *E. globulus*, OC kappa increased the level of growth-promoting hormones such as auxin, gibberellin and cytokinines in *E. globulus* trees (González et al., 2014b) as well as in pine trees (Saucedo et al., 2015). In addition, OC kappa increases the amount of volatile terpenes, and new terpenes having potential anti-pathogenic activities in *E. globulus* trees (González et al., 2014c). Thus, OC kappa mediated an increase in net photosynthesis, basal metabolism and secondary metabolism in *E. globulus* trees.

Considering that OC kappa increases net photosynthesis, the level of growth-promoting hormones, and basal and secondary metabolisms in plants, and that the activation of TOR

132 pathway lead to an increase in plant growth, photosynthesis, growth hormone level and basal an
133 secondary metabolisms in plants (see above), we hypothesize that OC kappa may induce an
134 increase in glucose and trehalose levels which may lead to an increase in G6P and T6P which
135 may inhibit SnRK1 which may increase the level of TOR-P which may lead to increase in
136 expression of genes encoding proteins of photosystems and enzymes involved in chlorophyll
137 synthesis, C, N and S assimilation, and PPCs and terpenes synthesis in *E. globulus* trees.

Materials and Methods

Plant culture, treatment with OC kappa and measurement of height

E. globulus trees were obtained from seeds produced by Semillas Imperial S.A. (Los Angeles, Chile). Plants having an initial height of approximately 30 cm (n=10 for each control and treated groups) were sprayed on leaves with water (control group) or with 5 mL of an aqueous solution containing OC kappa at a concentration of 1 mg mL⁻¹ once at the beginning of each week, four times in total, and cultivated outdoors in plastic bags containing composted soil for 17 additional weeks during spring and summer of 2015. Leaves (10 g) were obtained from the middle height part of control and treated trees, one day after each treatment, at the same time in the day (11 h in the morning), divided into three samples (n=3) and frozen in liquid nitrogen for further analyses. The height of *E. globulus* trees were determined using measuring tape.

Quantification of total chlorophyll

Quantification of chlorophylls *a* and *b* was performed as described in Lichtenthaler and Wellburn (1983). Fresh leaves (0.1 g) were frozen in liquid nitrogen and homogenized in a mortar with a pestle. One mL of acetone was added and the mixture was incubated at 4°C for 90 min. The mixture was centrifuged at 14.000 rpm for 5 min using a micro-centrifuge. The supernatant was recovered and the absorbance determined at 665 and 649 nm using a Hewlett Packard/Agilent spectrophotometer model 8453 (Santa Clara, CA, USA). Total chlorophyll was calculated by addition of chlorophylls *a* and *b* and the concentration of chlorophylls was calculated using the following formula:

$$\text{Chlorophyll } a \text{ (}\mu\text{g mL}^{-1}\text{)} = 13.96 A_{665} - 6.88 A_{649}$$

$$\text{Chlorophyll } b \text{ (}\mu\text{g mL}^{-1}\text{)} = 24.96 A_{665} - 7.32 A_{649}$$

Quantification of total reducing sugars

Quantification of total reducing sugars was performed as described in Hansen and Möller (1975). Fresh leaves (0.1 g) were frozen in liquid nitrogen and homogenized in a mortar. One mL of ethanol was added and the mixture centrifuged at 14.000 rpm for 5 min; the supernatant was then recovered. An aliquot of the supernatant (25 µL) was added to 475 µL of sulfuric anthrone solution prepared by mixing 150 mg of anthrone in 100 mL of sulfuric acid; the mixture was incubated at 60°C for 15 min. Absorbance was determined at 620 nm and the concentration

167 calculated using a calibration curve prepared with glucose at concentrations ranging from 0.065
168 to 0.5 mg mL⁻¹.

169 **Quantification of glucose**

170 Fresh leaves (0.1 g) were frozen in liquid nitrogen and homogenized in a mortar. Five hundred
171 µL of distilled water were added and the mixture centrifuged at 14.000 rpm for 5 min. The
172 supernatant was recovered and an aliquot of 30 µL was added to 500 µL of glucose
173 oxidase/peroxidase kit reaction mixture (Valtek Diagnostics, Santiago, Chile). The absorbance
174 was determined at 505 nm and the concentration was calculated using a calibration curve
175 prepared using glucose at concentrations of 0.2 to 2 mg mL⁻¹.

176 **Quantification of trehalose**

177 Quantification of trehalose was performed as described in Ahmed et al. (2013). Fresh leaves (0.1
178 g) were frozen in liquid nitrogen and homogenized in a mortar. Two mL of ethanol were added;
179 mixture was boiled for 1 h and ethanol was left to evaporate at 60° in an oven. Five mL of 5 mM
180 sulfuric acid were added and the mixture was centrifuged at 3.200 rpm for 10 min. The
181 supernatant was filtered through 0.2 µm pore PDVF filters and boiled in water for 1 h to
182 hydrolyze sucrose. Once cold, the pH was neutralized with sodium hydroxide, the solution
183 evaporated and the residue was dissolved in distilled water. The calibration curve was prepared
184 using trehalose at concentrations ranging 0 to 5 mg mL⁻¹.

185 **Preparation of protein extracts**

186 Protein extracts were prepared as described in Faurobert et al. (2007). Fresh leaves (1 g) were
187 frozen with liquid nitrogen and homogenized in a mortar. Three mL of extraction buffer (0.5 M
188 Tris-HCl, 0.7 M sucrose, 1 mM PMSF, 50 mM EDTA, 0.1 M KCl and 0.2% β-mercaptoethanol
189 pH 8.0) were added and the homogenate was shaken on ice for 10 min. One mL of phenol at pH
190 6.6-8.0 was added, the mixture was shaken on ice for 10 min and centrifuged at 3.200 rpm for 10
191 min at 4°C. The organic phase was recovered and mixed with 4 volumes of 0.1 M ammonium
192 acetate solubilized in methanol. The mixture was shaken using a vortex and incubated overnight
193 at -20°C for protein precipitation. The mixture was centrifuged at 3.200 rpm for 15 min at 4°C,
194 and the protein pellet was washed twice with ammonium acetate at 0.1 M in methanol, and then
195 once at the same concentration in acetone; the pellet was dried at room temperature and

solubilized in 50 mM Tris-HCl pH 8.0. Proteins were quantified using Bradford (1976) reagent and the calibration curve was prepared using bovine serum albumin.

Quantification of phosphorylated TOR (TOR-P)

Proteins (5 µg) were separated using a biphasic denaturant polyacrylamide gel (6% stacking phase and 12% resolving phase), and electrophoresis was performed at 110 V for 1.5 h. Proteins were electro-transferred to a nitrocellulose membrane using a TransBlot system (Bio-Rad) and 400 mA, at 4 °C for 1 h. The transfer of protein was verified by staining the membrane with Ponceau Red dye. The membrane was blocked with 5% skim milk solubilized in TTBS buffer (20 mM tris-HCl pH 7.5, 0.1 mM NaCl and 0.1% Tween 20), and washed three times with TTBS at room temperature for 10 min. The membrane was incubated with the monoclonal antibody anti-TOR-P Ser2448 (1:1000, Abcam ab109268) or anti-RbcL (1:2500, Agrisera AS03037) at room temperature for 1 h. The membrane was washed three times with TTBS at room temperature for 10 min, incubated with the secondary antibody anti-Rabbit IgG conjugated with HRP (Agrisera, AS09602) at room temperature for 1 h, and washed three times with TTBS at room temperature for 10 min. The membrane was incubated with a chemo-luminescent substrate (SuperSignal West Femto, Thermo Scientific, Rockford, IL, USA) for 5 min and was exposed to an X-ray film (Thermo Scientific, Rockford, IL, USA) for 3 min to detect TOR-P ser2448, or for 30 s to detect RbcL. Bands in the film were scanned and then quantified using Image Studio software (Li-Cor, USA).

RNA extraction

Total RNA was extracted from *Eucalyptus* leaves as described in Morante-Carriel et al. (2014). Fresh leaves (1 g) were frozen in liquid nitrogen and homogenized in a mortar with a pestle. Ten mL of solution A containing 100 mM Tris-HCl pH 8.0, 0.35 M sorbitol, 10% (w/v) polyethylenglycol 6000 and 2% (w/v) of β-mercaptoethanol were added and the mixture was shaken for 1 min. The mixture was centrifuged 3.500 rpm, at 4°C, for 15 min, and the supernatant was discarded. The pellet was solubilized in 10 mL of solution B containing 300 mM Tris-HCl pH 8.0, 25 mM EDTA, 2 M NaCl, 2% (w/v) CTAB, 0.05% (w/v) spermidine, 2% PVPP and 2% (w/v) β-mercaptoethanol; the mixture was heated at 65°C and incubated at 65°C for 10 min and shaken every 2 min using a vortex. A similar volume of a solution of chlorophorm/isoamyl alcohol (24:1) was added and the mixture was centrifuged at 3.200 rpm at 4°C for 10 min. The aqueous phase was extracted once more with a similar volume of chlorophorm/isoamyl alcohol

and centrifuged at 3.200 rpm at 4°C for 10 min. The aqueous phase was recovered and total RNA precipitated by addition of 0.1 volume of 0.3 M sodium acetate, pH 5.2, and 0.6 volumes of isopropanol; the mixture was incubated at -80°C for 30 min. The mixture was centrifuged at 14.000 rpm, at 4°C, for 20 min, and the supernatant discarded. The pellet was solubilized in 1 mL of nuclease free (DEPC-treated) water and total RNA was precipitated adding 0.3 volumes of 10 M lithium chloride; the mixture was incubated at 4°C overnight. The mixture was centrifuged at 13.000 rpm, at 4°C, for 30 min, and the supernatant was discarded. The pellet was solubilized in 0.1 mL of DEPC-treated water and total RNA precipitated adding 0.1 volume of 3 M sodium acetate pH 5.2, and 2 volumes of 70% cold ethanol; the mixture was centrifuged at 13.000 rpm at 4°C for 20 min, and the supernatant discarded. The pellet was washed with 200 µL of 70% cold ethanol and centrifuged at 13.000 rpm at 4°C for 10 min, and the supernatant discarded. The pellet was dried at room temperature and solubilized in 50 µL of DEPC-treated water. The concentration and purity of total RNA was determined measuring the absorbance at 260 and 280 nm, and in an agarose gel; RNA was stored at -80°C for further gene expression analyses.

Quantification of transcript levels by qRT-PCR

The relative level of transcripts was quantified by qRT-PCR using a real-time thermocycler Rotorgene 6000 (Corbett, Australia). Transcripts involved in glucose accumulation and consumption: were those encoding fructose-1,6-bisphosphatase 1 (*fbp1*), a key enzyme in glucose synthesis; α-amylase 3 (*amy3*), an important enzyme in starch degradation and glucose production; ADP-glucose pyrophosphorylase 1 (*apl1*), determinant enzyme in starch synthesis. Transcripts of proteins involved in TOR pathway were: TOR Kinase (*tor*), the regulatory kinase of TOR pathway; S6K (*s6k*), a kinase that is activated by TOR. Transcripts encoding photosystem proteins were: the subunit A of photosystem II (*psbA*), Rieske subunit of cytochrome b6f (*petC*), plastocyanin (*petE*), subunit A of photosystem I (*psaF*). Transcripts encoding enzymes were magnesium chelatase (*chlH*), a key enzyme of chlorophyll synthesis; the large subunit of ribulose-1,5-bisphosphate carboxylase/oxygenase (rubisco) (*rbcL*), a key enzyme in C assimilation; glutamine synthase (*gs1*), an enzyme involved in N assimilation; glutamate dehydrogenase (*gdh2*), an enzyme involved in N assimilation; O-acetylserine thiol-lyase (*cysK*), an enzyme involved in S assimilation; 5'-adenylsulfate reductase (*apr2*), an enzyme involved in S assimilation; phenylalanine ammonia-lyase 1 (*pall*), a key enzyme of phenylpropanoid pathway; and terpene synthase 1 (*ts1*), an enzyme involved in terpenes synthesis. RNA 18S was used as housekeeping gene. PCR primers are listed in Supplementary Table 1. qRT-PCR reactions

259 were performed using Sensimix One-step kit (Quantace, UK), 75 ng of total RNA, 200 nM
 260 primer solution and 3 mM magnesium chloride. Relative transcript level from three independent
 261 replicates was expressed as described by Livak and Schmittgen (2001) using the $2^{-\Delta\Delta CT}$ method.
 262 To this end, mean values of control samples were subtracted to mean values of treated samples to
 263 determine fold-change in expression.

264 **Statistical analyses**

265 Data were subject to one-way analysis of variance (ANOVA) and *post hoc* Tukey Test, previous
 266 to the evaluation of the requirements of normality and homogeneity of variance. Significant
 267 differences were estimated over 3 independent replicates at a 95% confidence interval.

268 Results

269 OC kappa-induced increases in levels of glucose and trehalose

270 *Eucalyptus* trees treated with OC kappa showed significant higher increase in height compared to
 271 controls, which started at week 9 and became more evident with time until week 21 (Fig. 1A).
 272 Treated trees showed an average height of 72 cm at week 21, whereas control trees showed an
 273 average height of 35 cm, indicating 105% higher increase in height in OC kappa-treated trees
 274 with respect to controls. In addition, trees treated with OC kappa showed a higher level of total
 275 chlorophylls starting at week 3 and remaining until week 11; the following week, the levels of
 276 total chlorophylls decreased to reach control levels in a continuing pattern until the end of the
 277 experiments (Fig. 1B). OC kappa showed no clear effects on the levels of total sugars if
 278 compared with controls; although there were a clear higher significant peaks in total sugar with
 279 respect to controls at week 12 and 20 (Fig. 1C). Furthermore, treated trees showed in general
 280 higher levels of glucose compared with controls; these differences were significant at weeks 1,
 281 from weeks 9-11, and from weeks 17-19 (Fig. 1D). Treated trees showed a trend of higher levels
 282 of trehalose if compared with controls with maximal level at weeks 1-3, 5, 8-9, 12, 15-16 and 18-
 283 21 (Fig. 1E).

284 OC kappa-induced levels of transcripts encoding enzymes involved in glucose accumulation

285 In order to analyze the reasons explaining the increases in the level of glucose induced by OC
 286 kappa, the level of transcripts encoding the enzymes fructose-1,6-bisphosphatase involved in
 287 glucose synthesis, *fbp1*; α -amylase 3 involved in starch degradation and production of glucose,
 288 *amy3*; and ADP-glucose pyrophosphorylase involved in starch synthesis, *apl1*, were detected.
 289 Trees treated with OC kappa showed an increase in the level of *fbp1* transcripts at weeks 3, 6, 8,
 290 10, 13 and 15 with respect to controls (Fig. 2A). Transcript levels of *amy3* peaked at weeks 1, 3,
 291 7-8, 10-12 and 16, compared to controls; peaks were the highest at weeks 7 and 11 (Fig. 2B).
 292 *Apl1* transcripts increased only at week 18 (Fig. 2C).

293 OC kappa-induced increase in the level of TOR-P and *tor* transcripts but not *s6k* transcripts

294 In order to analyze whether the increase in glucose and/or trehalose may induce the activation of
 295 TOR kinase, the level of TOR phosphorylated in ser2448 (active TOR-P) as well as that of the
 296 large subunit (RbcL) of the enzyme ribulose-1,5-bisphosphate carboxylase/oxygenase (rubisco)
 297 were detected using specific antibodies (Fig. 3A). The level of active TOR was normalized using

the level of RbcL (Fig. 3B). Trees treated with OC kappa showed a higher relative level of TOR-P from week 1 to the end of the experiment (week 21) and increases at weeks 1,2, 6, 12 and 16 (Fig. 3A-C). In order to detect whether the increase in active TOR-P is due to the increase in *tor* transcripts, the relative level of *tor* was detected. Trees treated with OC kappa showed peaks of increase in transcript levels encoding TOR kinase (*tor*) at weeks 3, 6, 10-11 and 13, compared to controls (Fig. 3C). In contrast, no significant changes were observed for transcripts encoding S6 kinase (*s6k*) throughout the experiments (Fig. 3D).

OC kappa-induced increase in the levels of transcripts encoding proteins involved in photosystems and chlorophyll synthesis

In order to analyze the reasons explaining the increase in net photosynthesis observed in previous works, the levels of transcripts of a subunit of photosystem (PS) II, *psbA*; the Rieske subunit of cytochrome b6f, *petC*; plastocyanin, *petE*; a subunit of PSI, *psaF*; and the enzyme magnesium chelatase involved in chlorophyll synthesis, *chlH*, were analyzed. Trees treated with OC kappa showed significant increase in the level of *psbA* transcripts at weeks 3-4, 8, 10-14 and 18 (Fig. 4A). Peaks of *petC* expression were observed to be significant at weeks 3-6, 10 and 17-18 (Fig. 4C). The increase of *petE* transcripts were significant at weeks 3, 5, 9-10, 14 and 18 (Fig. 4C). Expression of *psaF* was significantly higher at weeks 3, 10-11, 14 and 18 (Fig 4D). Finally, *chlH* transcripts increased significantly from weeks 5 to 15 (Fig. 4E).

OC kappa-induced increases in the level of transcripts encoding enzymes involved in C, N and S assimilation

In order to analyze the reasons explaining the increase in activities of enzymes involved in C, N and S assimilation observed in previous works, the level of transcripts encoding the large subunit of the enzyme rubisco involved in C assimilation, *rbcL*; the enzyme glutamine synthase (GlnS) involved in N assimilation, *gs1*; the enzyme glutamate dehydrogenase (GDH) involved in N assimilation, *gdh2*; the enzyme 5'-adenylsulfate reductase (APR) involved in S assimilation, *apr2*, and the enzyme O-acetylserine thiol-lyase (O-ASTL) involved in S assimilation, *cysK*. Treated trees showed a significant increase in *rbcL* transcripts at weeks 4, 6, 11 and 14 (Fig. 5A), in *gs1* at weeks 3-4, 7, 9-11, 13-14 and 18-19 (Fig. 5B), in *gdh2* at weeks 3-4, 6, 10 and 14 (Fig. 5C), in *apr2* at weeks 1, 3-4, 7 and 17 (Fig. 5D) and in *cysK* at weeks 3-6, 10, 14 and 17-18 (Fig. 5E).

OC kappa-induced increase in the level of transcripts encoding enzymes involved in secondary metabolism

In order to analyze the reasons explaining the increase in PPCs and terpenes induced by OC kappa and reported in previous works, the level of transcripts encoding enzyme phenylalanine ammonia-lyase (PAL) involved in PPCs synthesis, *pal*, and the enzyme terpene synthase involved in terpenes synthesis, *ts1*, were analyzed. Trees treated with OC kappa showed an increase in *pal1* transcripts at weeks 3, 6-7, 10 and 18 (Fig. 6A), and in *ts1* transcripts at weeks 3, 6 and 10-14 (Fig. 6B).

336 Discussion

337 OC kappa induced increases in the level of glucose and trehalose that are coincident with 338 increases in TOR-P increases but precedes the increase in transcript levels

339 In this work, we showed that treatment with OC kappa in *Eucalyptus* trees induced an initial
340 increase in glucose level at week 1 and in trehalose level at weeks 1-3. In addition, the increases
341 in glucose and trehalose are coincident with the initial increase in TOR-P observed at week 1-2
342 suggesting that the increases in these sugars could be related with phosphorylation and activation
343 of TOR kinase. In this respect, it has been shown that the increase in G6P and T6P inhibit SnrK1,
344 a kinase that inhibits TOR by phosphorylation, which results in TOR activation (Toroser et al.,
345 2000; Zhang et al., 2009). In addition, it has been shown that trehalose applied on leaves of wheat
346 induced an increase in growth suggesting that this increase results in the increase T6P levels
347 (Ibrahim et al., 2016). Thus, the increases in glucose and trehalose levels induced by OC kappa in
348 *E. globulus* trees may result in the increase in G6P and T6P levels that may inhibit snRK1 that, in
349 turn, may trigger the increase in active TOR-P leading to the stimulation of growth. Furthermore,
350 OC kappa induced additional increases in glucose level at weeks 9-11 and 17-19. Moreover, the
351 level of transcripts encoding enzymes leading to glucose accumulation, fructose-1,6-
352 biphosphatase and α -amylase, increased weeks 1, 3, 7-8, 10-11, 13, 15 and 16. The latter
353 suggests that the increase in glucose level may be due, at least in part, to the increase in the level
354 of transcripts of enzymes that produce glucose.

355 On the other hand, the increases in trehalose level showed an oscillatory pattern with
356 peaks at weeks 1-3, 5, 8-9, 12, 15-16 and 18-21 which correlates with the increase in the level of
357 transcripts encoding proteins of PS and enzymes of basal and secondary metabolisms observed at
358 weeks 3-4, 5-6, 10-11, and in some cases at weeks 13-14 and 16-18. In this sense, it has been
359 shown that activation of different isoforms of trehalose 6-P synthase (TPS), the enzyme that
360 produces trehalose, can be activated by snRK1 and/or by calcium-dependent protein kinases,
361 CDPKs (Glinski and Weckwert, 2005). Thus, the oscillatory pattern observed in T6P level, TOR-
362 P and transcripts encoding proteins involved in photosynthesis, and basal and secondary
363 metabolisms, may be explained by the activation of CDPKs that increases trehalose and T6P
364 levels inhibiting SnRK1 and activating TOR kinase. In this sense, it is important to mention that
365 *Eucalyptus* plants treated with 50 μ M rapamycin or 250 μ M AZ8055 did not show growth
366 inhibition (data not shown) but they displayed greater height compared to the controls.

367 Consequently, *Eucalyptus* trees might have alternative pathways different from snRK1/TOR
368 pathway, probably involving CDPKs.

369 **OC kappa-induced increase in the level of TOR-P and *tor* transcripts but not *s6k* transcripts**

370 OC kappa increases in the level of TOR-P from week 1 until the end of the experiment (week 21)
371 with peaks at weeks 1, 2, 6, 12 and 16 compare to control plants. In this sense, it has been shown
372 that an insulin-like growth factor (zmIGF) as well as bovine insulin induced an increase in cell
373 division and growth in maize callus, phosphorylation of TOR in ser2448 and S6K in thr389
374 (Garrocho-Villegas et al., 2013). In addition, it was shown that rapamycin inhibited TOR and
375 S6K phosphorylations. Thus, growth stimulation induced by zmIGF and insulin in maize is due
376 to the activation of TOR pathway involving phosphorylation of TOR and S6K. In addition, it was
377 shown that zmIGF interact with a receptor located in the plasma membrane of maize cells
378 (Garrocho-Villegas et al., 2013). Therefore, it is possible that OC kappa may interact with a
379 receptor located in the plasma membrane leading to the production inositol 1,4,5 triphosphate
380 (IP₃) which induces release of calcium from ER activating CDPKs and the latter may may
381 activate enzymes that produced G6P and T6P which inhibit SnRK1 leading to TOR activation
382 explaining, at least in part, the stimulation of growth observed in *E. globulus* trees (see model in
383 Fig. 7). On the other hand, it was determined that the level of *tor* transcripts showed increases at
384 weeks 3, 6, 10-11 and 13 whereas *s6k* transcripts levels did not change. Thus, OC kappa induce
385 an increase expression of *tor* gene expression indicating that TOR level is transcriptionally-
386 regulated and the increase in TOR could be related to the increase in TOR-P level.

387 **OC kappa-induced increases in the level of transcripts encoding proteins of photosystems** 388 **and chlorophyll synthesis**

389 OC kappa induced an increase in the levels of transcripts encoding proteins of PS II and I which
390 may explain, at least in part, the increase in net photosynthesis previously observed in *E.*
391 *globulus* trees (González et al., 2014a; González et al., 2013a). In this sense, it has been shown
392 that the inhibition of TOR with AZD8055 leads to a decrease in transcripts encoding proteins
393 involved in photosynthesis, chlorophyll synthesis (Dong et al. 2015) indicating that the activation
394 of TOR pathway leads to the increase photosynthesis. In addition, the levels of transcripts
395 encoding PS proteins showed an oscillatory pattern. As mentioned before, OC kappa may activate
396 CDPKs that may phosphorylate enzymes that synthesize G6P and T6P synthase leading to an
397 increase in G6P and T6P levels which may inhibit SnRK1 leading to TOR activation, resulting in

the increase in genes encoding proteins involved in photosynthesis and chlorophyll synthesis, thus, increasing growth in *E. globulus* trees (see model in Fig. 7). On the other hand, OC kappa induced and increase in total chlorophyll observed at weeks 3-11 and this increase partially overlaps with the higher expression of magnesium chelatase, a key enzyme in chlorophyll synthesis, which increases at weeks 5-15. Thus, the increase in chlorophyll level may occur due to an increased expression of enzymes involved in chlorophyll synthesis.

OC kappa-induced increase in the level of transcripts encoding enzymes of basal and secondary metabolism

Treatment of *Eucalyptus* with OC kappa induced higher expression of genes involved in C, N and S assimilation which is in accord with previous results showing an increase in activities of enzymes involved in C assimilation, rubisco; in N assimilation, GlnS and GDH; and in S assimilation, APR and O-ASTL in *E. globulus* trees (González et al., 2014a). In addition, transcripts encoding enzymes involved in secondary metabolism, PAL and TPS, also increased in response to OC kappa. The latter explain previous results obtained *E. globulus* trees treated with OC kappa showing an increase in PPCs levels (González et al., 2013b) as well as in volatile terpenes (González et al., 2014b). These results may indicate that the increased activities of enzymes involved in C, N and S assimilation as well as the increase in the level of PPCs and terpenes is due to the increase in expression of the genes encoding enzymes involved in basal and secondary metabolism in *Eucalyptus* trees treated with OC kappa. Moreover, the increase in expression of enzymes involved in basal and secondary metabolisms also showed an oscillatory pattern. As mentioned before, OC kappa may induce the release of calcium from ER which may activate CDPKs that may activate enzymes that synthesize G6P and T6P which may inhibit snRK1 and activate TOR which may lead to activation of transcription regulatory factors resulting in the increase in expression of genes encoding enzymes involved in basal and secondary metabolism resulting in an enhancement of growth and defense responses in *E. globulus* trees (see model in Fig. 7).

Conclusions

E. globulus trees treated with OC kappa displayed an initial increase in glucose and trehalose levels at week 1-3, an increase in the level of TOR-P at week 1-2 and an increase in the level of transcripts encoding proteins involved in photosynthesis and enzymes related to chlorophyll synthesis, and C, N and S assimilation, and associated with the syntheses of PPCs and terpenes,

beginning at weeks 3-4 and displaying an oscillatory pattern. Thus, OC kappa may induce an increase in glucose (G6P) and trehalose (T6P) levels which may inhibit SnRK1 leading to the activation of TOR pathway which may induce the increase in expression of genes involved in photosynthesis, basal metabolism and secondary metabolisms, leading to the enhanced in growth and defense responses in *E. globulus* trees (see model in Fig. 7).

Acknowledgments

This work was funded by Sirius Natura S.A. and VRIDEI-USACH. Silvia Saucedo was financed by SENECYT-Ecuador, Convocatoria 2011.

References

- Acosta-Jaquez HA, Keller JA, Foster KG, Ekim B, Soliman G.A, Feener BP, Ballif BA, Fingar DC (2009) Site-specific mTOR phosphorylation promotes mTORC1-mediated signaling and cell growth. *Mol Cell Biol* 29:4308-4324. <https://doi.org/10.1128/MCB.01665-08>
- Ahmed HE, Elhousseiny AY, Maimona AK, Qaid EA (2013) Trehalose accumulation in wheat plant promotes sucrose and starch biosynthesis. *Jord J Biol Sci* 6:143-150. <https://doi.org/10.12816/0000272>
- Banaszynski LA, Liu CW, Wandless TJ (2005) Characterization of FKBP.rapamycin.FRB ternary complex. *J Am Chem Soc* 127:4715-4721. <https://doi.org/10.1021/ja043277y>
- Baretic D, Berndt A, Ohashi Y, Johnson CM, Williams RL (2016) TOR forms a dimer through an N-terminal helical solenoid with a complex topology. *Sci Rep* 7:11016. <https://doi.org/10.1038/ncomms11016>
- Bosotti R, Isacchi A, Sonhammer EL (2000) FAT: a novel domain in PIK-related kinases. *Trends Biochem Sci*. 25:225-227. [https://doi.org/10.1016/S0968-0004\(00\)01563-2](https://doi.org/10.1016/S0968-0004(00)01563-2)
- Bradford MM (1976) A rapid and sensitive method for quantification of microgram quantities of protein utilizing the principle of protein-dye binding. *Anal Biochem* 72:248-254. [https://doi.org/10.1016/0003-2697\(76\)90527-3](https://doi.org/10.1016/0003-2697(76)90527-3)
- Caldana C, Li Y, Leisse A, Zhang L, Bartholomaeus L, Fernie AR, Willmitzer L, Giavalisco P (2013) Systemic analysis of inducible target of rapamycin reveals a general metabolic switch controlling growth in *Arabidopsis thaliana*. *Plant J* 73:897-899. <https://doi.org/10.1111/tpj.12080>
- Castro J, Vera J, González A, Moenne A (2012) Oligo-carrageenans stimulate growth by enhancing photosynthesis, basal metabolism, and cell cycle in tobacco plants (var. Burley). *J Plant Growth Regul* 31:173-185. <https://doi.org/10.1007/s00344-011-9229-5>
- Chiang GG, Abraham RT (2005) Phosphorylation of mammalian Target of Rapamycin (mTOR) at Ser-2448 is mediated by p70S6 kinase. *J Biol Chem* 280:25485-25490. <https://doi.org/10.1074/jbc.M501707200>
- Crespo JL, Díaz-Troya S, Florencio FJ. 2005. Inhibition of target of rapamycin signaling by rapamycin in the unicellular green alga *Chlamydomonas reinhardtii*. *Plant Physiol* 139:1736-1749. <https://doi.org/10.1104/pp.105.070847>
- Dames SA. 2010. Structural bases for the association of the redox-sensitive target of rapamycin FATC domain with membrane-mimetic micelles. *J Biol Chem* 285:7766-7776. <https://doi.org/10.1074/jbc.M109.058404>

- 470 Deng K, Yu L, Zheng X, Zhang K, Wang W, Dong P, Zhang J, Ren M. 2016. Target of
471 Rapamycin is a key player for auxin signaling transduction in *Arabidopsis*. Front Plant Sci 7,
472 article 291. <https://doi.org/10.3389/fpls.2016.00291>
- 473 Deprost D, Yao L, Sormani R, Moreau M, Leterreux G, Nicolai M, Bedu M, Robaglia C, Meyer
474 C. 2007. The *Arabidopsis* TOR kinase links plant growth, yield, stress resistance and mRNA
475 translation. EMBO Rep 8:864-870
- 476 Dobrenel T, Caldana C, Hanson J, Robaglia C, Vincent M, Veit B, Meyer C. 2016. TOR signaling
477 and nutrient sensing. Annu Rev Plant Biol 67:24.1-24. [https://doi.org/10.1146/annurev-](https://doi.org/10.1146/annurev-arplant-043014-114648)
478 arplant-043014-114648
- 479 Dong P, Xiong F, Que Y, Wang K, Yu L, Li Z (2015) Expression profiling and functional analysis
480 reveals that TOR is a key player in regulating photosynthesis and phytohormone signaling
481 pathways in *Arabidopsis*. Front Plant Sci 6: article 677.
482 <https://doi.org/10.3389/fpls.2015.00677>
- 483 Faurobert M, Pelpoir E, Chaïb J (2007) Phenol extraction of proteins for proteomic studies of
484 recalcitrant plant tissues. In Plant Proteomics, Methods and Protocols. Humana Press, New
485 Jersey, USA. <https://doi.org/10.1385/1597452270>
- 486 Garrocho-Villegas V, Aguilar R, Sanchez de Jimenez E (2013) Insights into TOR-S6K pathway in
487 maize (*Zea mays* L.) pathway activation by effector-receptor interaction. Biochemistry 52,
488 9129-9140. <https://doi.org/10.1021/bi401474x>
- 489 Glinski M., Weckwerth W (2005) Differential multisite phosphorylation of the trehalose-6-
490 phosphate synthase gene family in *Arabidopsis thaliana*. Mol Cell Proteomics 4: 1614-1625.
491 <https://doi.org/10.1074/mcp.M500134-MCP200>
- 492 González A, Castro J, Vera J, Moenne A (2013a) Seaweed oligosaccharides stimulate plant
493 growth by enhancing carbon and nitrogen assimilation, basal metabolism and cell division. J
494 Plant Growth Regul 32:443-448. <https://doi.org/10.1007/s00344-012-9309-1>
- 495 González A, Contreras RA, Moenne A (2013b) Oligo-carrageenans enhance growth and content
496 of cellulose, essential oils and polyphenolic compounds in *Eucalyptus globulus* trees.
497 Molecules 18:8740-8751. <https://doi.org/10.3390/molecules18088740>
- 498 González A, Moenne F, Gómez M, Sáez CA, Contreras RA, Moenne A (2014a) Oligo-
499 carrageenan kappa increases NADPH, ascorbate and glutathione syntheses and TRR/TRX
500 activities enhancing photosynthesis, basal metabolism, and growth in *Eucalyptus* trees. Front
501 Plant Sci 5: article 512. <https://doi.org/10.3389/fpls.2014.00512>

- 502 González A, Contreras Ra, Zuñiga G, Moenne A (2014b) Oligo-carrageenan kappa-induced
503 reducing redox status and activation of TRR/TRX system increase the level of indole-3-acetic
504 acids, gibberellin A3 and *trans*-zeatin in *Eucalyptus globulus* trees. *Molecules* 19:12690-
505 12698. <https://doi.org/10.3390/molecules190812690>
- 506 González A, Gutierrez-Cutiño M, Moenne A (2014c) Oligo-carrageenan kappa-induced reducing
507 redox status and increase in TRR/TRX activities promote activation and reprogramming of
508 terpenoid metabolism in *Eucalyptus* trees. *Molecules* 19:7356-7367.
509 <https://doi.org/10.3390/molecules19067356>
- 510 Hansen J, Möller I (1975) Percolation of starch and soluble carbohydrates from plant tissue for
511 quantitative determination with anthrone. *Anal Biochem* 68:87-94.
512 [https://doi.org/10.1016/0003-2697\(75\)90682-X](https://doi.org/10.1016/0003-2697(75)90682-X)
- 513 Halford NG, Hey SJ (2009) Snf1-related protein kinases (SnRKs) act within an intricate network
514 that links metabolic and stress signaling in plants. *Biochem J* 419:247-259.
- 515 Ibrahim HA, Abdellatif YMR (2016) Effect of maltose and trehalose on growth, yield and some
516 biochemical components in wheat plant under water stress. *Ann Agric Sci* 61: 267-274.
517 <https://doi.org/10.1016/j.aoas.2016.05.002>
- 518 Jang JC, León P, Zhou L, Sheen J. (1997) Hexokinase as sugar sensor in higher plants. *Plant Cell*
519 9:5-19
- 520 Jewell JL, Kim YC, Russell RC, Yu FX, Park HW, Plouffe SW, Tagliabracci CS, Guan KL (2015)
521 Differential regulation of mTORC1 by leucine and glutamine. *Science* 347:194-198.
522 <https://doi.org/10.1126/science.1259472>
- 523 Kang SA, Pacold ME, Cervantes CL, Lim D, Lou HJ, Ottina K, Gray NS, Turk BE, Yaffe MN,
524 Sabatini DM (2013) mTORC1 phosphorylation sites encode their sensitivity to starvation and
525 rapamycin. *Science* 341:1236566
- 526 Kim DH, Sarbassov DD, Ali SM, King, JE, Latek RR, Erdjument-Bromage H, Tempst B,
527 Sabatini DM (2002) mTOR interacts with Raptor to form a nutrient-sensitive complex that
528 signals to the cell growth machinery. *Cell* 110:163-175. [https://doi.org/10.1016/S0092-](https://doi.org/10.1016/S0092-8674(02)00808-5)
529 [8674\(02\)00808-5](https://doi.org/10.1016/S0092-8674(02)00808-5)
- 530 Kim YK, Kim S, Shin YJ, Hur YS, Kim, WY, Lee MS, Cheon CL, Verma DP (2014) Ribosomal
531 protein S6, a target of rapamycin, is involved in the regulation of rRNA genes by possible
532 epigenetic changes in *Arabidopsis*. *J Biol Chem* 289:391-3912
- 533 Kunz J, Schneider U, Howald I. Schmidt A, Hall MN (2000) HEAT repeats mediate plasma
534 membrane localization of Tor2p in yeast. *J Biol Chem* 275:37011-37020

- 535 Lichtenthaler HK, Wellburn AR (1983) Determinations of total carotenoids and chlorophylls *a*
536 and *b* of leaf extracts in different solvents. Biochem Soc Trans 11:591-592.
537 <https://doi.org/10.1042/bst0110591>
- 538 Livak KJ, Schmittgen TD. 2001. Analysis of relative gene expression data using real-time
539 quantitative PCR and the 2(-Delta Delta C(T)) Method. Methods. 25:402-408.
540 <https://doi.org/10.1006/meth.2001.1262>
- 541 Mahfouz MM, Kim S, Delaunay AJ, Verma DP (2006) *Arabidopsis* TARGET OF RAPAMYCIN
542 interacts with RAPTOR, which regulates the activity of S6 kinase in response to osmotic stress
543 signals. Plant Cell 18:477-490. <https://doi.org/10.1105/tpc.105.035931>
- 544 Martin DE, Hall MN (2005) The expanding TOR signaling network. Curr Opin Cell Biol 17:158-
545 166. <https://doi.org/10.1016/j.ceb.2005.02.008>
- 546 Moenne A (2016) Marine algae oligo-carrageenans (OCs) stimulate growth and defense
547 responses in terrestrial plants. In Research Progress in Oligosaccharins. Springer, New York,
548 USA. <https://doi.org/10.3390/molecules18088740>
- 549 Montané MH, Menand B (2013) ATP-competitive mTOR kinase inhibitors delay plant growth by
550 triggering early differentiation of meristem cells but not developmental patterning change. J
551 Exp Bot 64:4361-4374. <https://doi.org/10.1093/jxb/ert242>
- 552 Morante-Carriel J., Sellés-Marchart S, Martínez-Márquez A, Martínez-Esteso MJ, Luque I, Bru-
553 Martínez R (2014) RNA isolation from loquat and other recalcitrant woody plants with high
554 quality and yield. Anal Biochem 452:46-53. <https://doi.org/10.1016/j.ab.2014.02.010>
- 555 Moreau M, Azoppari M, Clément G, Dobrenel T, Marchive C, Renne C, Martin-Magniette DL,
556 Taconnat L., Renou JP, Robaglia C, Meyer C (2012). Mutation in the *Arabidopsis* homolog of
557 LST8/G β L, a partner of Target of Rapamycin kinase, impair plant growth, flowering, and
558 metabolic adaptation to long days. Plant Cell 24:463-481.
559 <https://doi.org/10.1105/tpc.111.091306>
- 560 Nukarinen E, Hägele T, Pedrotti L, Wurzinger B, Mair A, Landgraf R, Börnke F, Hanson J, Teige
561 M., Baena-González E, Dröge-Laser W, Weckwerth W (2016) Quantitative phosphoproteomic
562 reveals the role of AMPK plant ortholog snRK1 as a metabolic master regulator under energy
563 deprivation. Sci Rep 6, 31697. <https://doi.org/10.1038/srep31697>
- 564 Ren M, Qiu S, Venglat P, Xiang D, Feng L, Selvaraj G, Datla R (2011) Target of Rapamycin
565 regulates development and ribosomal RNA expression through kinase domain in *Arabidopsis*.
566 Plant Physiol 155:1367-1382. <https://doi.org/10.1104/pp.110.169045>

- 567 Ren M, Venglat P, Qiu S, Feng L, Cao Y, Wang E, Xiang D, Wang J, Alexander D, Chalivendra S,
568 Logan D, Matoo A, Selvaraj G, Datla R (2012) Target of rapamycin signaling regulates
569 metabolism, growth, and life span in *Arabidopsis*. Plant Cell 24:4850-4874.
570 <https://doi.org/10.1105/tpc.112.107144>
- 571 Rexin D, Meyer C, Robaglia C, Veit B (2015) TOR signalling in plants. Biochem J 470:11-14.
572 <https://doi.org/10.1042/BJ20150505>
- 573 Rodriguez-Camargo DC, Link NM, Dames SA (2012) The FKBP12-rapamycin binding domain
574 of human TOR undergoes strong conformational changes in the presence of membrane
575 mimetics with and without the regulator phosphatidic acid. Biochemistry 51:4909-4921.
576 <https://doi.org/10.1021/bi3002133>
- 577 Sarbassov DD, Ali SM, Kim DH, Guertin DA, Latek RR, Erdjument-Bromage H, Tempst T,
578 Sabatini DM (2004) Rictor, a novel binding partner of mTOR, defines a rapamycin-insensitive
579 and raptor-independent pathway that regulates the cytoskeleton. Curr Biol 14:1296-1302.
580 <https://doi.org/10.1016/j.cub.2004.06.054>
- 581 Sarbassov DD, Guertin DA, Ali SM, Sabatini DM (2005) Phosphorylation and regulation of
582 Akt/PKB by the rictor mTOR complex. Science 307:1098-1101.
583 <https://doi.org/10.1126/science.1106148>
- 584 Saucedo S, Contreras RA, Moenne A (2015) Oligo-carrageenan kappa increases C, N, and S
585 assimilation, auxin and giberellin contents, and growth in *Pinus radiata* trees. J Forest Res
586 26:635-640. <https://doi.org/10.1007/s11676-015-0061-9>
- 587 Schalm SS, Fingar DC, Sabatini DM, Blenis J (2003) TOS motif-mediated raptor binding
588 regulates 4E-BP1 multisite phosphorylation and binding. Curr. Biol. 13:797-806.
589 [https://doi.org/10.1016/S0960-9822\(03\)00329-4](https://doi.org/10.1016/S0960-9822(03)00329-4)
- 590 Sormani R, Yao L, Menand B, Ennar N, Lecampion C., Meyer C, Robaglia C (2007)
591 *Saccharomyces cerevisiae* FKBP12 binds *Arabidopsis thaliana* TOR and its expression in
592 plants leads to rapamycin susceptibility. BMC Plant Biol 7:26. [https://doi.org/10.1186/1471-](https://doi.org/10.1186/1471-2229-7-26)
593 [2229-7-26](https://doi.org/10.1186/1471-2229-7-26)
- 594 Takahashi T, Hara K, Inoue H, Kawa Y, Tokunawa C, Hidayat S, Yoshino K, Kuroga Y,
595 Yonezawa K (2000) Carboxyl-terminal region conserved among phosphoinositides-kinase-
596 related kinases is indispensable for mTOR function *in vivo* and *in vitro*. Genes Cells 5:765-
597 775. <https://doi.org/10.1046/j.1365-2443.2000.00365.x>
- 598 Toroser D, Plaut Z, Huber SC (2000) Regulation of plant SNF-related protein kinase by glucose-
599 6-P. Plant Physiol 123:403-411. <https://doi.org/10.1104/pp.123.1.403>

- 600 Vera J, Castro J, González A, Moenne A (2011) Seaweed polysaccharides and derive
601 oligosaccharides stimulate defense responses and protection against pathogens in plants. *Mar*
602 *Drugs* 9:2514-2525. <https://doi.org/10.3390/md9122514>
- 603 Wullschlegel S, Loewith R, Hall MN (2006) TOR signaling in growth and metabolism. *Cell*
604 124:471-484. <https://doi.org/10.1016/j.cell.2006.01.016>
- 605 Xiong Y, Sheen J (2012) Rapamycin and glucose-target of rapamycin (TOR) protein signaling in
606 plants. *J Biol Chem* 287:2836-2842. <https://doi.org/10.1074/jbc.M111.300749>
- 607 Xiong Y, McCormack L, Li L, Hall K., Xiang, C., and Sheen, J. (2013) Glc-TOR signalling lead
608 to transcriptome re-programming and meristem activation. *Nature* 496:181-186.
609 <https://doi.org/10.1038/nature12030>
- 610 Xiong Y, Sheen J (2013) Moving beyond translation. *Cell Cycle* 13:1989-1990.
611 <https://doi.org/10.4161/cc.25308>
- 612 Xiong Y, Sheen J (2015) Novel links in the TOR plant kinase signaling networks. *Curr Opin Plant*
613 *Biol* 28:83-91. <https://doi.org/83-91>. 10.1016/j.pbi.2015.09.006
- 614 Yang H, Rudge DG, Koos JD, Vaidialingam B, Yang HJ, Pavletich NP (2013) mTOR kinase
615 structure, mechanism and regulation. *Nature* 497:217-223
- 616 Zhang Y, Primavesi LF, Jhurea D, Androljic PJ, Mitchell RA, Powers SJ, (2009) Inhibition of
617 SNF1-related protein kinase 1 activity and regulation of metabolic pathways by trehalose-6-
618 phosphate. *Plant Physiol* 149:1860-1871. <https://doi.org/10.1104/pp.108.133934>
- 619

620 Figure legends

621 **Figure 1.** Increase in height (A), level of total chlorophyll (B), total reducing sugars (C), glucose
622 (D) and trehalose (E) in control (open circles) and in *E. globulus* trees treated with OC kappa at 1
623 mg mL⁻¹ (black circles). The increase in height is expressed in centimeters, the level of total
624 chlorophyll is expressed in micrograms per gram of fresh tissue and the level of total reducing
625 sugars, glucose and trehalose are expressed in milligram per gram of fresh tissue. Numbers over
626 circles highlight weeks when the most important peaks were observed. Within each experimental
627 week, asterisks (*) indicate when there are significant differences ($p < 0.05$) between OC kappa-
628 treated and control trees. Circles represent the mean value of three independent triplicates \pm SD.

629 **Figure 2.** Relative level of transcripts encoding enzymes fructose-1,6-bisphosphatase (*fbp1*, A),
630 amylase (*amy3*, B), and ADP-glucose pyrophosphorylase (*apl1*, C) in control and in *E. globulus*
631 trees treated with OC kappa at 1 mg mL⁻¹. Asterisks (*) represent significant differences ($p <$
632 0.05) between the level of transcripts at a certain week compared with the expression at the
633 beginning of the experiments (week 0). Relative level of transcripts is expressed as $2^{-\Delta\Delta Ct}$. Circles
634 represent the mean value of three independent triplicates \pm SD.

635 **Figure 3.** Level of active TOR kinase (TOR-P ser4448), and large subunit of ribulose-1,5-
636 bisphosphate carboxylase/oxygenase (RbcL) in control (A) and in *E. globulus* trees treated with
637 OC kappa at 1 mg mL⁻¹ (B). Levels of active TOR (C) are expressed in relative units of band
638 intensity corresponding to the ratio TOR/RbcL. Relative level of transcripts encoding TOR kinase
639 (*tor*, D) and S6 kinase (*s6k*, E) in control and *E. globulus* trees treated with OC kappa at 1 mg
640 mL⁻¹. Numbers over circles highlight weeks when the most important parameter peaks were
641 observed. For Fig. 3C, within each experimental week, asterisks (*) indicate when there are
642 significant differences ($p < 0.05$) between OC kappa-treated and control trees. For Fig. 3D-F,
643 asterisks (*) represent significant differences ($p < 0.05$) between the level of transcripts at a
644 certain week compared with the expression at the beginning of the experiments (week 0). The
645 level of transcripts is expressed as $2^{-\Delta\Delta Ct}$. Circles represent mean values of three independent
646 experiments \pm SD.

647 **Figure 4.** Relative level of transcripts encoding subunit A of photosystem II (*psbA*, A), subunit
648 Rieske of cytochrome b6f (*petC*, B), plastocyanin (*petE*, C), subunit F pf photosystem I (*psaF*, D)

and magnesium chelatase (*chlH*, E), in control (open circles) and *E. globulus* trees treated with OC kappa at 1 mg mL⁻¹ (black circles) Asterisks (*) represent significant differences ($p < 0.05$) between the level of transcripts at a certain week compared with the expression at the beginning of the experiments (week 0). The level of transcripts is expressed as $2^{-\Delta\Delta C_t}$. Circles represent mean values of three independent experiments \pm SD.

Figure 5. Relative level of transcripts encoding the large subunit of ribulose-1,5-carboxylase/oxygenase (*rbcL*, A), glutamine synthase (*gs1*, B), glutamate dehydrogenase (*gdh2*, C), 5'-adenylsulfate reductase (*apr2*, D) and O-acetylserine thiol-lyase (*cysK*, D) in control (open circles) and *E. globulus* trees treated with OC kappa at 1 mg mL⁻¹ (black circles). Asterisks (*) represent significant differences ($p < 0.05$) between the level of transcripts at a certain week compared with the expression at the beginning of the experiments (week 0). The level of transcripts is expressed as $2^{-\Delta\Delta C_t}$. Circles represent mean values of three independent experiments \pm SD.

Figure 6. Relative level of transcripts encoding phenylalanine ammonia-lyase (*pall*, A) and terpene synthase (*ts1*, B), in control and in *E. globulus* trees treated with OC kappa at 1 mg mL⁻¹ (black circles). Asterisks (*) represent significant differences ($p < 0.05$) between the level of transcripts at a certain week compared with the expression at the beginning of the experiments (week 0). The level of transcripts is expressed as $2^{-\Delta\Delta C_t}$. Circles represent mean values of three independent experiments \pm SD.

Figure 7. Proposed model of OC kappa-induced signaling in *E. globulus*. OC kappa binds to a membrane-associated receptor (Receptor), potentially coupled to a G protein (G); this may activate phospholipase C (PLC) leading to the release of inositol 1,4,5 triphosphate (IP₃) which may activate an IP₃-dependent channel in the endoplasmic reticulum (ER) leading to the calcium release; calcium may activate calcium dependent protein kinases (CDPKs) which, in turn, may activate enzymes that synthesize G6P and T6P. The increases in G6P and T6P levels may inhibit SnRK1 leading to the activation of TOR kinase. Then TOR may mediate the activation of transcription factors (TF) leading to the increase in expression of genes encoding proteins of photosystems and enzymes of basal metabolism, enhancing plant growth, as well as enzymes of secondary metabolism increasing defenses responses in *E. globulus* trees.

Figure 1

Increase in growth and status of photosynthesis and sugars

Increase in height (A), level of total chlorophyll (B), total reducing sugars (C), glucose (D) and trehalose (E) in control (open circles) and in *E. globulus* trees treated with OC kappa at 1 mg mL⁻¹ (black circles). The increase in height is expressed in centimeters, the level of total chlorophyll is expressed in micrograms per gram of fresh tissue and the level of total reducing sugars, glucose and trehalose are expressed in milligram per gram of fresh tissue. Numbers over circles highlight weeks when the most important peaks were observed. Within each experimental week, asterisks (*) indicate when there are significant differences ($p < 0.05$) between OC kappa-treated and control trees. Circles represent the mean value of three independent triplicates \pm SD.

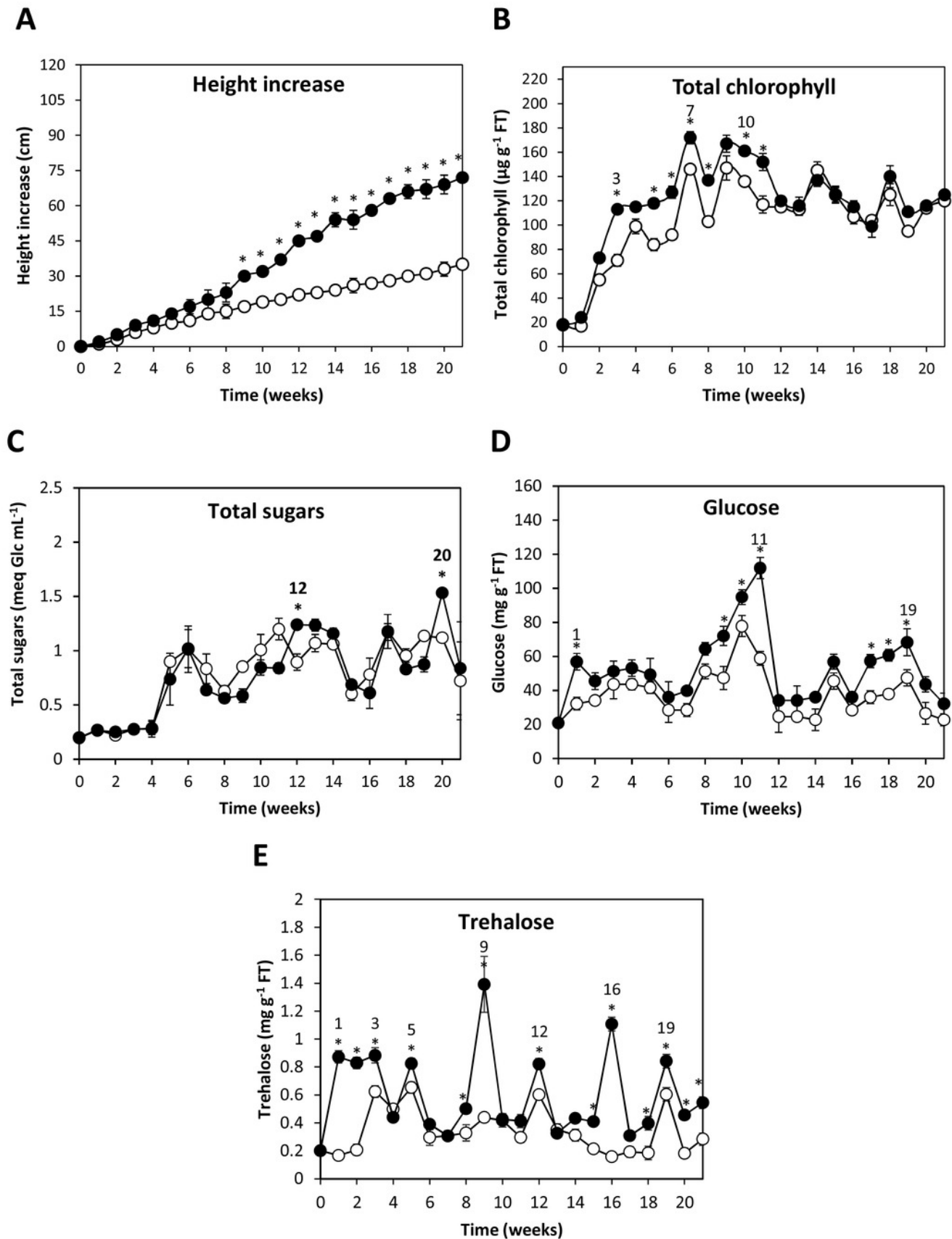


Figure 2

Transcript levels of sugar metabolism genes

Relative level of transcripts encoding enzymes fructose-1,6-bisphosphatase (*fbp1*, A), amylase (*amy3*, B), and ADP-glucose pyrophosphorylase (*apl1*, C) in control and in *E. globulus* trees treated with OC kappa at 1 mg mL⁻¹. Asterisks (*) represent significant differences ($p < 0.05$) between the level of transcripts at a certain week compared with the expression at the beginning of the experiments (week 0). Relative level of transcripts is expressed as $2^{-\Delta\Delta Ct}$. Circles represent the mean value of three independent triplicates \pm SD.

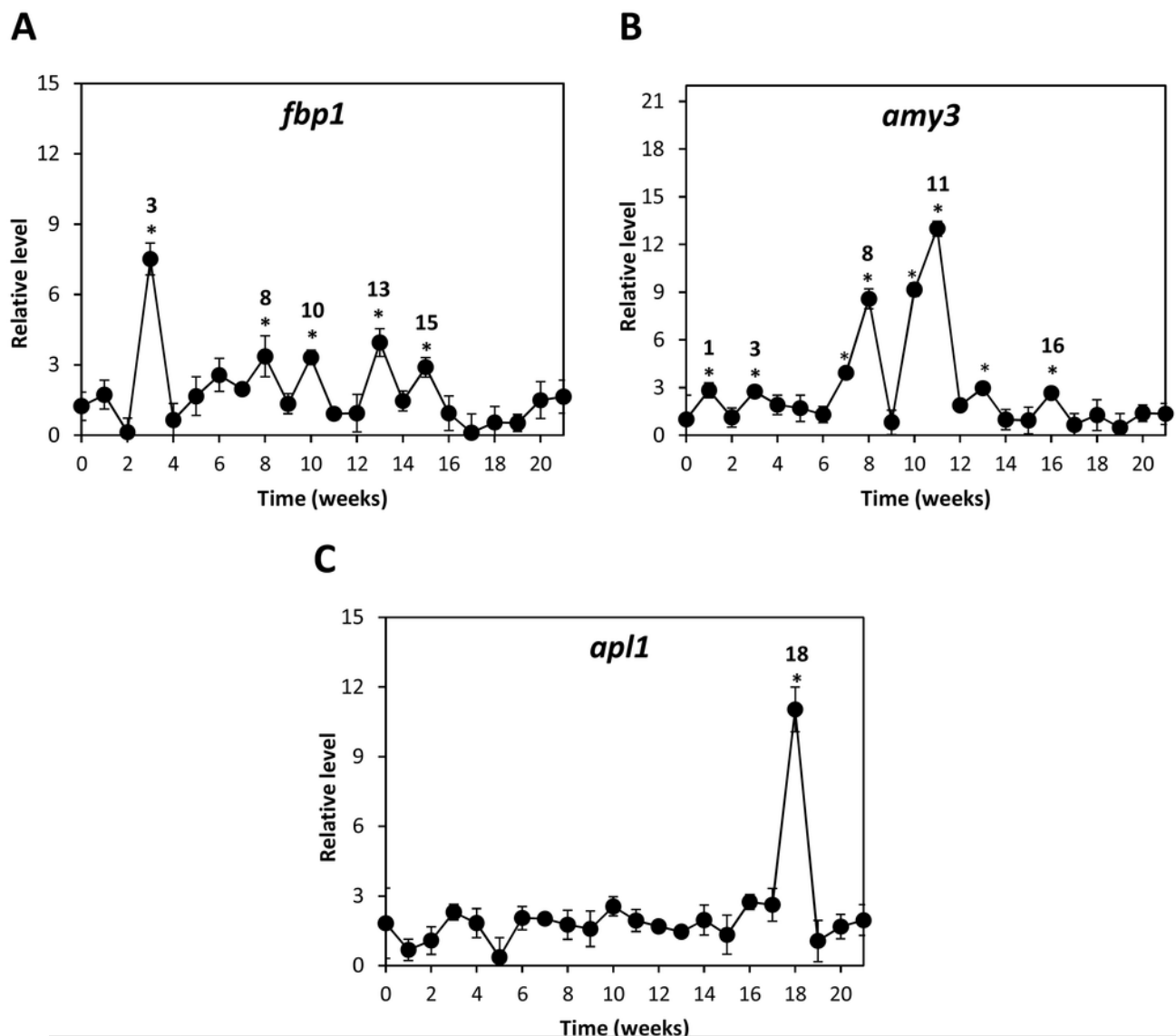
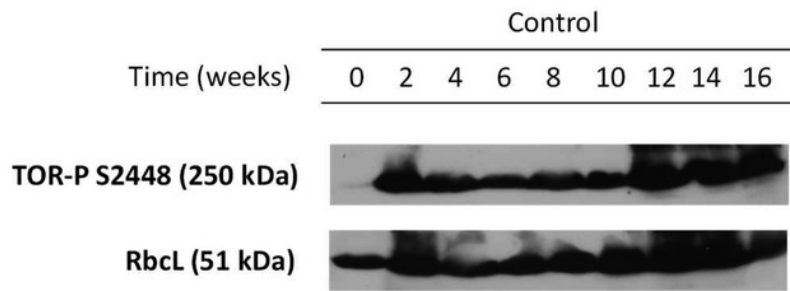


Figure 3

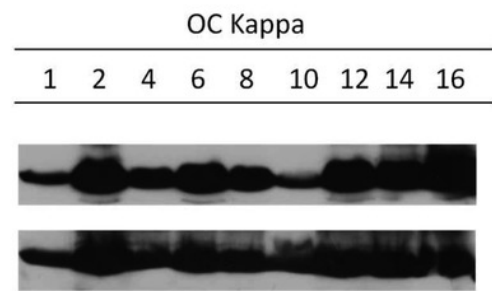
Activation of TOR kinase induced by OC kappa

Level of active TOR kinase (TOR-P ser4448), and large subunit of ribulose-1,5-bisphosphate carboxylase/oxygenase (RbcL) in control (A) and in *E. globulus* trees treated with OC kappa at 1 mg mL⁻¹ (B). Levels of active TOR (C) are expressed in relative units of band intensity corresponding to the ratio TOR/RbcL. Relative level of transcripts encoding TOR kinase (*tor*, D) and S6 kinase (*s6k*, E) in control and *E. globulus* trees treated with OC kappa at 1 mg mL⁻¹. Numbers over circles highlight weeks when the most important parameter peaks were observed. For Fig. 3C, within each experimental week, asterisks (*) indicate when there are significant differences ($p < 0.05$) between OC kappa-treated and control trees. For Fig. 3D-F, asterisks (*) represent significant differences ($p < 0.05$) between the level of transcripts at a certain week compared with the expression at the beginning of the experiments (week 0). The level of transcripts is expressed as $2^{-\Delta\Delta Ct}$. Circles represent mean values of three independent experiments \pm SD.

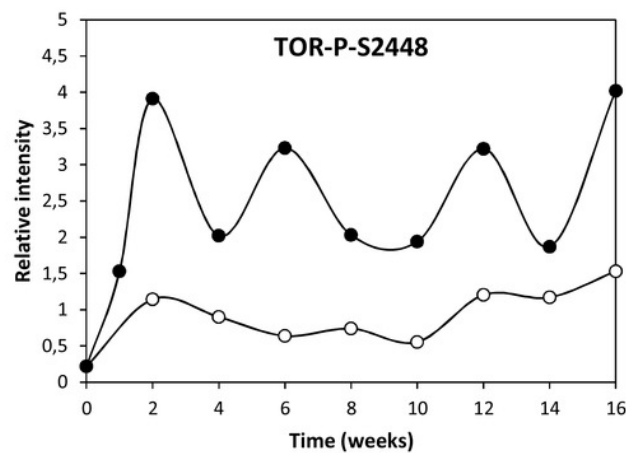
A



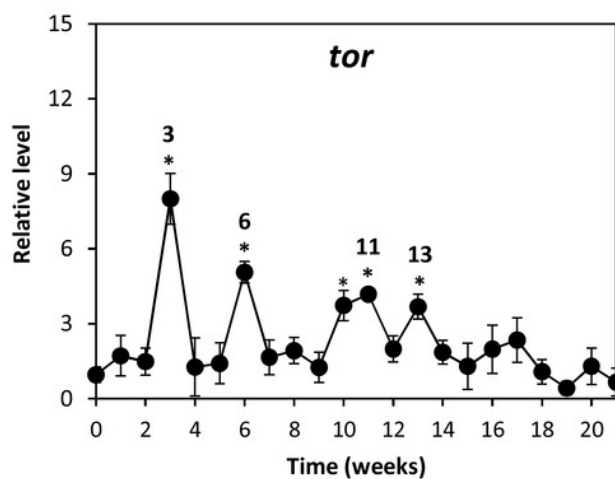
B



C



D



E

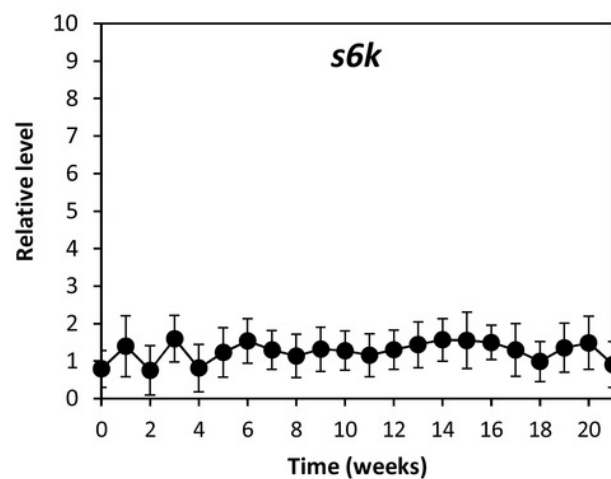
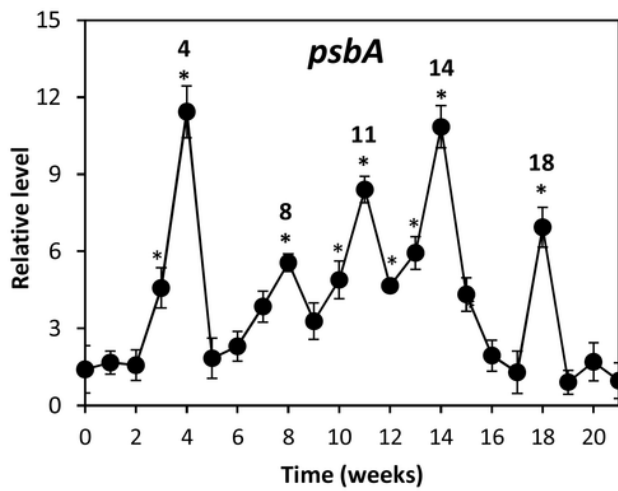


Figure 4

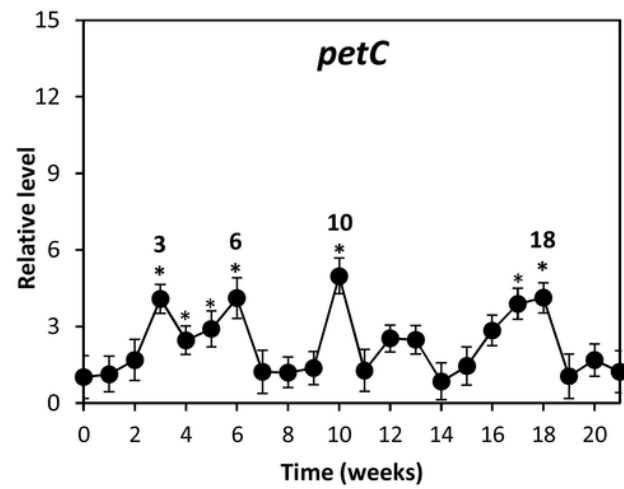
Transcript levels of photosynthesis related genes

Relative level of transcripts encoding subunit A of photosystem II (*psbA*, A), subunit Rieske of cytochrome b6f (*petC*, B), plastocyanin (*petE*, C), subunit F of photosystem I (*psaF*, D) and magnesium chelatase (*chlH*, E), in control (open circles) and *E. globulus* trees treated with OC kappa at 1 mg mL⁻¹ (black circles) Asterisks (*) represent significant differences ($p < 0.05$) between the level of transcripts at a certain week compared with the expression at the beginning of the experiments (week 0). The level of transcripts is expressed as $2^{-\Delta\Delta C_t}$. Circles represent mean values of three independent experiments \pm SD.

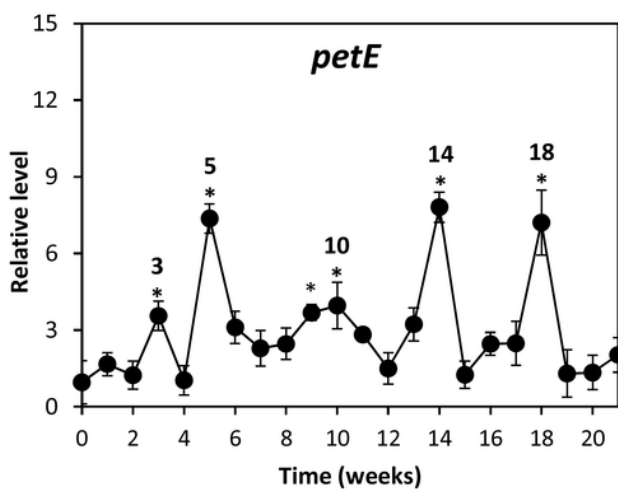
A



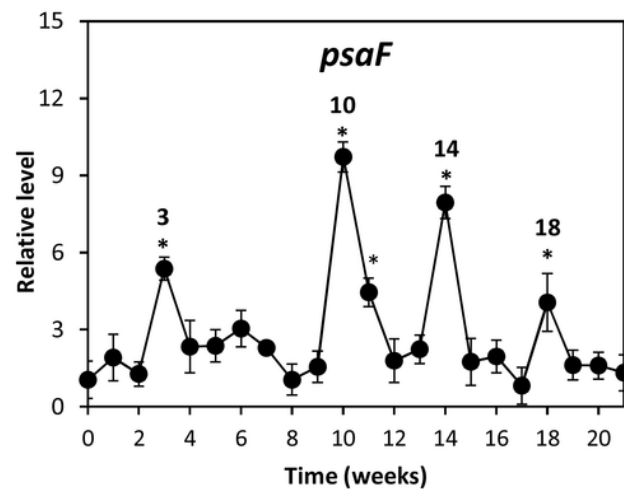
B



C



D



E

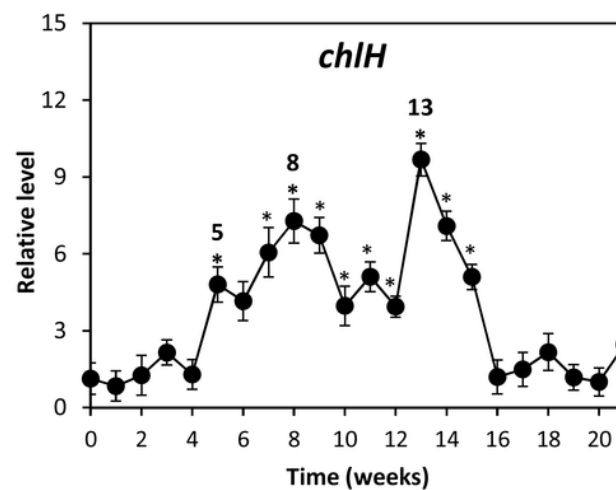
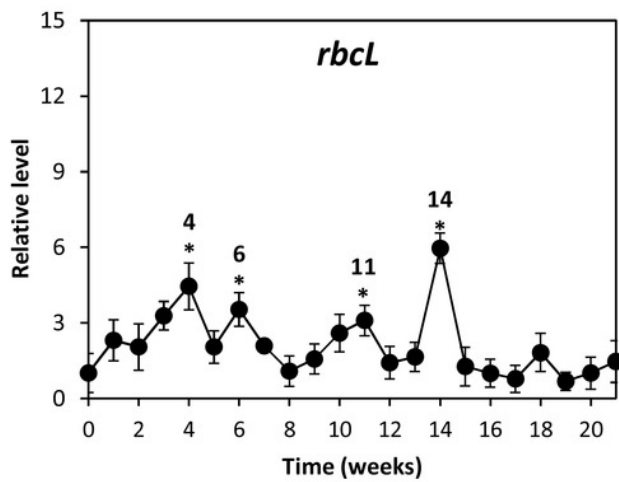


Figure 5

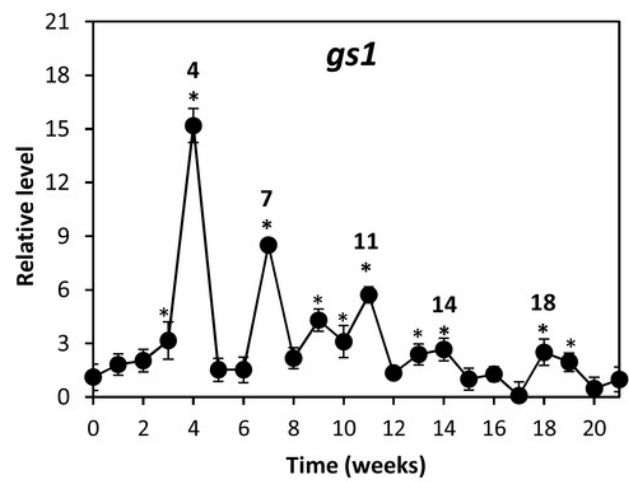
Transcript levels of carbon, nitrogen and sulfur assimilation related genes

Relative level of transcripts encoding the large subunit of ribulose-1,5-carboxylase/oxygenase (*rbcL*, A), glutamine synthase (*gs1*, B), glutamate dehydrogenase (*gdh2*, C), 5'-adenylsulfate reductase (*apr2*, D) and O-acetylserine thiol-lyase (*cysK*, D) in control (open circles) and *E. globulus* trees treated with OC kappa at 1 mg mL⁻¹ (black circles). Asterisks (*) represent significant differences ($p < 0.05$) between the level of transcripts at a certain week compared with the expression at the beginning of the experiments (week 0). The level of transcripts is expressed as $2^{-\Delta\Delta Ct}$. Circles represent mean values of three independent experiments \pm SD.

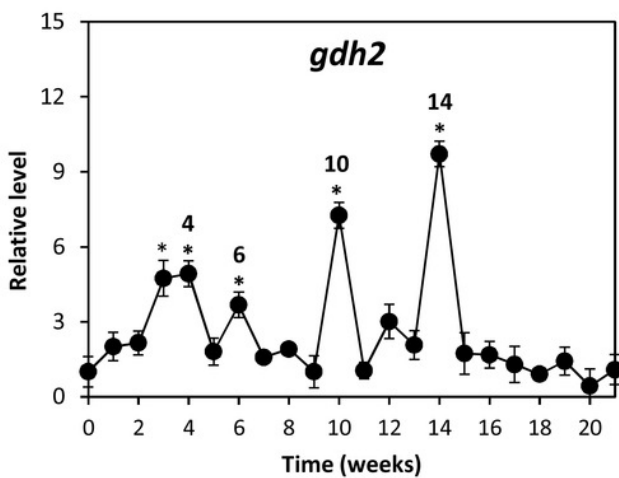
A



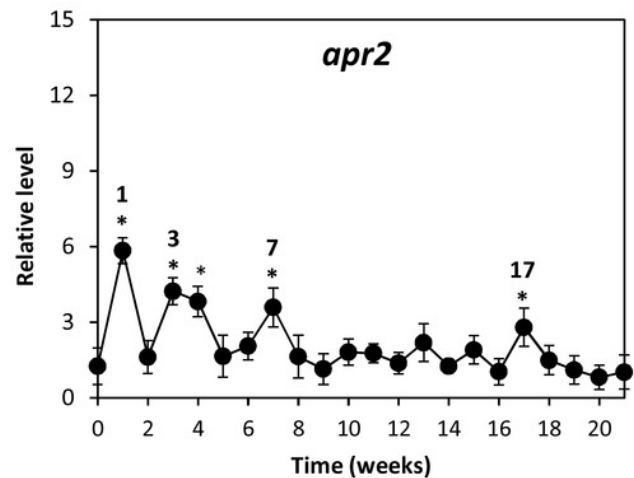
B



C



D



E

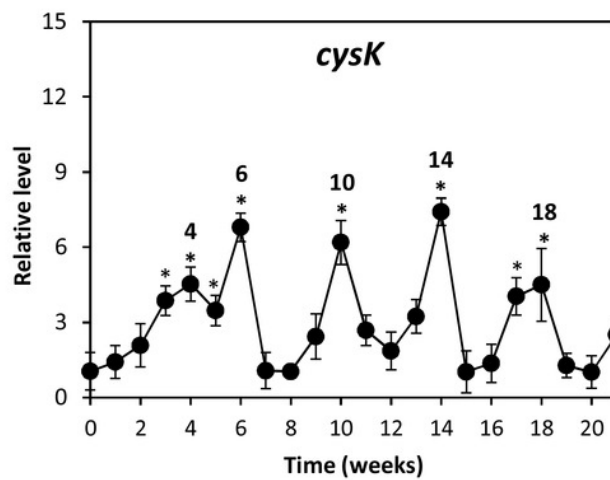


Figure 6

Transcript levels of secondary metabolism related genes

Relative level of transcripts encoding phenylalanine ammonia-lyase (*pal1*, A) and terpene synthase (*ts1*, B), in control and in *E. globulus* trees treated with OC kappa at 1 mg mL⁻¹ (black circles). Asterisks (*) represent significant differences ($p < 0.05$) between the level of transcripts at a certain week compared with the expression at the beginning of the experiments (week 0). The level of transcripts is expressed as $2^{-\Delta\Delta Ct}$. Circles represent mean values of three independent experiments \pm SD.

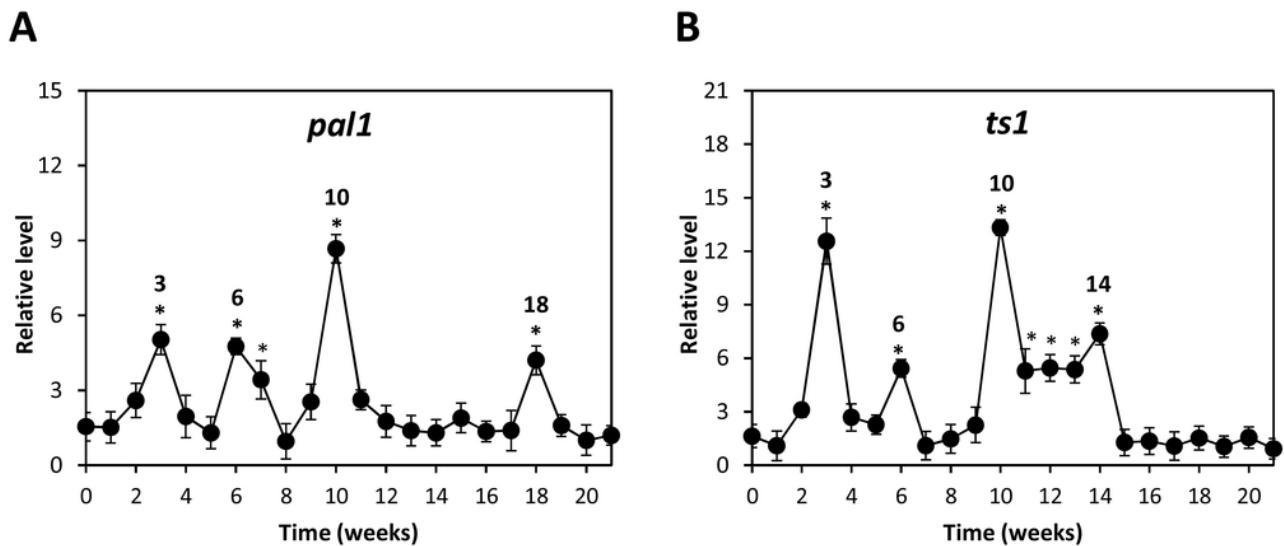


Figure 7

Proposed model of OC kappa-induced signaling in *E. globulus*

OC kappa binds to a membrane-associated receptor (Receptor), potentially coupled to a G protein (G); this may activate phospholipase C (PLC) leading to the release of inositol 1,4,5 triphosphate (IP_3) which may activate an IP_3 -dependent channel in the endoplasmic reticulum (ER) leading to the calcium release; calcium may activate calcium dependent protein kinases (CDPKs) which, in turn, may activate enzymes that synthesize G6P and T6P. The increases in G6P and T6P levels may inhibit SnRK1 leading to the activation of TOR kinase. Then TOR may mediate the activation of transcription factors (TF) leading to the increase in expression of genes encoding proteins of photosystems and enzymes of basal metabolism, enhancing plant growth, as well as enzymes of secondary metabolism increasing defenses responses in *E. globulus* trees.

